Icarus 211 (2011) 1150–1161

Contents lists available at ScienceDirect

Icarus

journal homepage: www.elsevier.com/locate/icarus

Are Phobos and Deimos the result of a giant impact?

Robert A. Craddock

Center for Earth and Planetary Studies, National Air and Space Museum, MRC-315, Smithsonian Institution, Washington, DC 20560, United States

ARTICLE INFO

Article history:
Received 16 April 2010
Revised 29 October 2010
Accepted 29 October 2010
Available online 6 November 2010

Keywords:
Mars
Mars, Satellites
Satellites, Formation
Impact processes

ABSTRACT

Despite many efforts an adequate theory describing the origin of Phobos and Deimos has not been realized. In recent years a number of separate observations suggest the possibility that the martian satellites may have been the result of giant impact. Similar to the Earth–Moon system, Mars has too much angular momentum. A planetesimal with 0.02 Mars masses must have collided with that planet early in its history in order for Mars to spin at its current rate (Dones, L., Tremaine, S. [1993]. Science 259, 350–354). Although subject to considerable error, current crater-scaling laws and an analysis of the largest known impact basins on the martian surface suggest that this planetesimal could have formed either the proposed 10,600 by 8500-km-diameter Borealis basin, the 4970-km-diameter Elysium basin, the 4500-km-diameter Daedalia basin or, alternatively, some other basin that is no longer identifiable. It is also probable that this object impacted Mars at a velocity great enough to vaporize rock (>7 km/s), which is necessary to place large amounts of material into orbit. If material vaporized from the collision with the Mars-spinning planetesimal were placed into orbit, an accretion disk would have resulted. It is possible that as material condensed and dissipated beyond the Roche limit forming small, low-mass satellites due to gravity instabilities within the disk. Once the accretion disk dissipated, tidal forces and libration would have pulled these satellites back down toward the martian surface. In this scenario, Phobos and Deimos would have been among the first two satellites to form, and Deimos the only satellite formed—and preserved—beyond synchronous rotation. The low mass of Phobos and Deimos is explained by the possibility that they are composed of loosely aggregated material from the accretion disk, which also implies that they do not contain any volatile elements. Their orbital eccentricity and inclination, which are the most difficult parameters to explain easily with the various capture scenarios, are the natural result of accretion from a circum-planetary disk.

Published by Elsevier Inc.

1. Introduction

Since their discovery in 1877, determining the origin of Phobos and Deimos has remained problematic. Spectral analyses suggest that the composition of Phobos closely matches black or carbonaceous chondrites (e.g., Murchie et al., 1991). This combined with other physical properties such as their low densities (the latest estimate is $\sim 1.860 \pm 0.060$ g/cm^3 for Phobos and -1.650 ± 0.3 g/cm^3 for Deimos; Rosenblatt et al., 2008) and low geometric albedoes ($\sim$0.06–0.07; Lynch et al., 2007) has led many investigators to suggest that they are captured asteroids (e.g., Burns, 1978; Forget et al., 2008). However, the orbits of both moons are extremely circular and their Laplace plane is very close to the martian equatorial plane. Captured objects would be expected to have elongate orbits with randomly oriented orbital planes. Phobos may have been able to attain its circular orbit because it experiences tidal perturbations due to its closeness to Mars, which are aided by libration. However, Deimos is too far away to experience much of either. Integration of Phobos' present eccentricity into the past indicates that it would have collided with Deimos (Lambeck, 1979). A number of ad hoc alternatives have been proposed to save the capture theory, including circularization of their orbits from atmospheric drag induced by an extended martian protoatmosphere (Pollack et al., 1979) or fragmentation of a single large captured satellite during the period of heavy bombardment (Hartmann et al., 1975; Safronov et al., 1986; Landis, 2002; Singer, 2007). However, in the former scenario the protoatmosphere would have to be in place long enough to circularize the orbits of the satellites but removed before the resulting drag pulled the satellites down to the martian surface. In the latter scenario, referred to as "co-accretion," (Burns, 1992) the distribution of particle sizes caused by fragmentation of the captured object would follow a power-law relation with the largest object approaching $\sim$85% the size of the original object (Hartmann et al., 1975). Reaccretion of this material would occur within a few hundred orbits (Soter, 1971), and it is unlikely that only two objects the size of Phobos and Deimos would remain. Also, reaccretion of the smaller particles into several objects would result in a satellite composed of

E-mail address: craddockb@si.edu

0019-1035/$ - see front matter Published by Elsevier Inc.
doi:10.1016/j.icarus.2010.10.023

many different sized blocks. However, analysis of Phobos' libration (Lambeck, 1979) suggests that this satellite is composed of homogenous material. Analysis of the impact history of Phobos through smooth particle hydrodynamic code modeling (Asphaug and Benz, 1994) also supports the idea that this satellite is composed of homogenous material probably <500 m in diameter.

An alternative hypothesis that is frequently overlooked is the possibility that Phobos and Deimos are the result of a giant impact. Such an idea was first suggested by Singer (1966), who proposed that Phobos and Deimos may have been "kicked" off the martian surface by a meteorite impact. Strom et al. (1992) also suggested that material was placed into orbit following the formation of the 7700-km-diameter Borealis basin forming a swarm of satellites that once orbited Mars. Schultz and Lutz-Garihan (1982, 1988) and Schultz (1985) came to a similar conclusion based on their analyses that Mars has a statistically large number of oblique impact craters on the surface that could be explained by the grazing impacts of former moonlets. However, Bottke et al. (2000) reassessed the oblique crater populations on Mars using a higher value of the threshold angle below which impact craters become elliptical (θ_{thresh} of 12° versus 5° as suggested by Schultz and Lutz-Garihan (1982)), and determined that there is no such excess population of elliptical craters compared to the Moon and Venus, and that most of the oblique impact craters on Mars were formed by asteroids. The possibility that some of the oblique craters on Mars were formed by the impact of former moonlets remains, however. More recently, Chappelow and Herrick (2008) analyzed a double, oblique impact feature north of Acheron Fossae at 40°N, 222.5°E (Fig. 1) and determined that the most likely object to have formed it is a former Mars-orbiting moonlet whose orbit tidally decayed.

The other lines of evidence that Phobos and Deimos are the result of a giant impact come from analyses of the spins of the terrestrial planets, which suggest that Mars, like the Earth, has too much prograde angular momentum to be explained by the accretion of many small bodies (Dones and Tremaine, 1993). Simply stated, the spin rate of Mars can only be explained by a collision with a planetesimal during accretion (Dones and Tremaine, 1993). The number of impact basins on Mars support the idea that large objects struck its surface early in its history, including evidence that a giant impact formed the Borealis basin and created the martian dichotomy (Wilhelms and Squyres, 1984; Andrews-Hanna et al., 2008). Could one of these giant collisions have placed enough material into orbit to form Phobos, Deimos, and other potential moonlets as well?

The purpose of this manuscript is to synthesize various ideas investigators have had about not only the Mars system but the Earth–Moon system as well. As such, it is meant to be speculative, but it is also meant to be thought provoking. The hypothesis that Phobos and Deimos formed from a giant impact has merit and deserves further attention from various disciplines within the planetary science community.

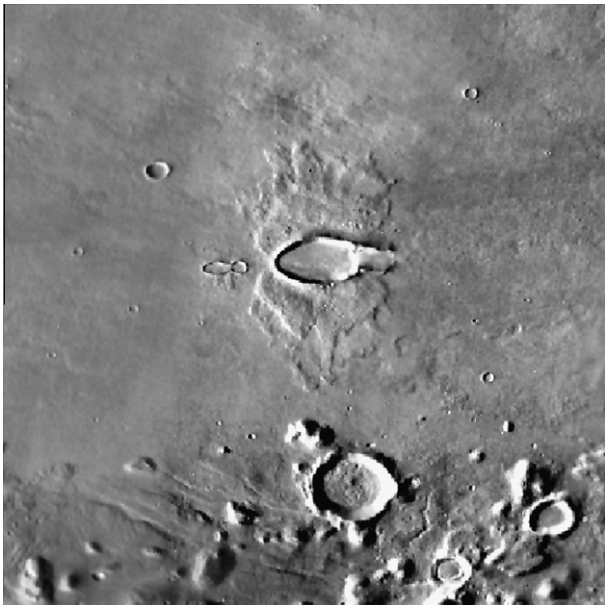

Fig. 1. A double, oblique impact crater located at 40.5°N, 222.5°E north or Archeon Fossae. Although the origin of such elliptical impact craters on Mars is uncertain, Chappelow and Herrick (2008) determined that the nature of these particular features is best explained by the impact of a former Mars-orbiting moonlet. Potentially many such moonlets were in orbit around Mars at one time, and Phobos and Deimos are the only two surviving objects.

2. The spin rate of Mars

An indirect line of evidence suggesting the possibility that Phobos and Deimos originated from a giant impact comes from analyses of the martian spin rate and assessment of the effects a giant impact might have based on current crater-scaling laws. From Dones and Tremaine (1993), the spin rate of a planet is expressed as the number of sidereal rotations per revolution around the Sun, $\mathfrak{R}$ and is written as

$$\mathfrak{R} = \frac{3\langle l_z \rangle}{2\Omega R_p^2} \tag{1}$$

where l_z is the specific angular momentum perpendicular to the orbital plane, Ω is the planet's orbital frequency (1.06×10^{-7} rad/s), and R_p is the planetary radius of Mars (3.39×10^6 m). The assumption made is that the dimensionless parameter r remains constant during accretion. This parameter is defined as

$$r \equiv \frac{R_p}{R_H} \equiv \frac{R_p}{(GM_p/\Omega^2)^{1/3}} \tag{2}$$

where R_H is the Hill, or tidal, radius of the planet, G is the universal gravitational constant ($6.6.73 \times 10^{-11}$ m^3 kg^{-1} s^{-2}), and M_p is the mass of the planet (6.43×10^{23} kg). The Hill radius is simply the distance where centrifugal force balances the gravitational attraction from the planet. For Mars, $\mathfrak{R} = 670$ and is a positive value because Mars rotates in a prograde direction and $r = 0.0022$.

If a planet is formed by the accretion of many small bodies, a process referred to as ordered accretion, then a maximum prograde or retrograde spin rate is possible. Dones and Tremaine (1993) show that with ordered accretion, values for $\mathfrak{R}r$ should be between −2.2 and 0.3. However, $\mathfrak{R}r = 1.5$ for Mars, which they argue is evidence that the rotation of Mars resulted from a stochastic component or, in other words, is the result of stochastic accretion. In stochastic accretion a planet's final spin rate is determined by the imperfect cancellation of angular momentum between individual impactors. Simply, a single impactor more massive than the rest determines the final rotation rate and direction of the planet. They show that the typical rotation rate can be estimated from the equation

$$|\mathfrak{R}| \approx \frac{S_m}{r^{3/2}} \approx \frac{m_1}{M_p} r^{-3/2} \tag{3}$$

where S_m is the dimensionless effective mass of a planetesimal relative to the planet, m_1 is mass of a single impactor, which is more massive than all the rest, and M_p is the mass of the planet. From this equation, it follows that

$$S_m = \frac{m_1}{M_p} \tag{4}$$

For stochastic accretion and a planet spinning prograde Dones and Tremaine (1993) show that

$$S_m \geqslant 0.3r^{1/2} \quad (5)$$

For Mars, $S_m \geqslant 0.015$, which implies that the minimum mass of the planetesimal (m_1) which induced the present spin rate of Mars, is $\sim 9.6 \times 10^{21}$ kg. Assuming such an object had a density of ~ 3 g/cm^3 its diameter would be $\sim$1800 km. A planetesimal with such a diameter is plausible. The accretion theory calculations performed by Hartmann and Davis (1975) indicated that a Mars-sized object formed near the proto-Earth and eventually collided with our planet. These calculations became the impetus for the giant impact hypothesis, which is now the paradigm for creation of the Moon (e.g., Wood, 1986). What is often overlooked, however, is that Hartmann and Davis (1975) also predict a Moon-sized object ($\sim$1800 km in diameter) forming near proto-Mars. Large impacts are recorded on the surface of Mars, and it may be possible that the collision with the Mars-spinning object is recorded as one of the larger proposed impact basins. Analyses of these basins can provide clues to the possible impact velocity and incidence angle of this collision.

2.1. Proposed martian basins and total impact energy

The largest proposed impact basin on Mars is located in Borealis. Wilhelms and Squyres (1984) first proposed a 7700-km-diameter impact basin to explain the martian dichotomy boundary, but the lack of a raised rim and the inability to fit a circular basin to the irregular dichotomy boundary weakened this hypothesis (Frey and Schultz, 1988; McGill and Squyres, 1991). More recently Andrews-Hanna et al. (2008) analyzed the gravity and topography of Mars to locate the dichotomy boundary under Tharsis and determined that the entire boundary can be fitted by an ellipse measuring 10,600 km by 8500 km centered at 67°N, 208°E. Other proposed large impact basins include Elysium (4970-km-diameter; Schultz and Frey, 1990), Daedalia (4500-km-diameter; Craddock et al., 1990), and Utopia (3300-km-diameter; McGill, 1989). Because these impacts are so old (>4.0 GY) and extensively modified, they are typically poorly defined. Evidence for their existence varies, but it generally consists of topographic lows, circular occurrences of massifs or kipukas, related geologic units (e.g., interior volcanic flows), or radial or circumferential fractures. For comparison, the largest well-defined impact basin on Mars, Hellas, is only $\sim$1800 km in diameter. Potentially other large diameter basins may exist on Mars; however, analyses of the currently available data have only identified those listed above.

To determine whether any of these impacts were capable of inducing Mars to spin, an estimate of the impactor mass, m_1, or its impact velocity, v, must be made. This can be calculated by knowing the total impact energy, W. Presently three different scaling relations exist which allow one to estimate W from the crater diameter. Because of the imprecision in determining the impact energy, however, all of these relations must be considered. They are discussed only briefly here, but an excellent review is presented in Melosh (1989, pp. 112–121).

The oldest relation has its foundations in the Cold War and nuclear explosion testing at the Nevada test site. Nordyke (1962) derived a scaling relation equating crater diameter to explosion depth and yield. However, because this relation was derived from terrestrial explosion data it corresponds to $g = 980$ cm/s^2 and is not directly applicable to craters formed in the martian environment.

Gault (1974) and Gault and Wedekind (1977) derived scaling relations experimentally using the Vertical Gun Facility at NASA's Ames Research Center. To estimate the amount of kinetic energy released during the formation of the Borealis basin, Wilhelms and Squyres (1984) adopted a modified equation based on these experiments where

$$D = KW^a h(g) \quad (6)$$

D is the diameter of the impact basin, K and a are constants (c.g.s units), W is the total amount of kinetic energy released, and $h(g) = g^{-1/6}$, where g is surface gravity (370 cm/s^2). In situations involving large, basin-sized impacts on planets gravitational strength dominates and $a = 0.29$ (Gault and Wedekind, 1977; Housen et al., 1979). A value of $K = \sim 7.0 \times 10^{-2}$ was used by Wilhelms and Squyres (1984), which is appropriate for describing a weak target such as regolith. In this study, however, a value of $K = 4.2 \times 10^{-2}$ was used. This assumes that the surface of Mars is a strong target, specifically basalt (Housen et al., 1979), and is arguably a more appropriate value especially for describing large, basin-forming impacts in the early crust of Mars.

Holsapple and Schmidt (1980, 1982) used the principal of dimensional invariance to develop scaling rules for impact cratering. Simply stated, different physical characteristics that describe the impact cratering event are grouped together to form dimensionless parameters. Experiments determine the functional dependence of a particular parameter on the others. This approach is referred to as π-group scaling after the "π-theorem" devised by E. Buckingham in 1914. Melosh (1989, p. 121) has shown that the π-group scaling relation for impacts occurring in competent rock can be expressed as

$$D = 1.8\rho_i^{0.11}\rho_t^{-1/3}g^{-0.22}L^{0.13}W^{0.22} \quad (7)$$

where ρ_i and ρ_t are the densities of the impactor and the target material (i.e., the surface of Mars), respectively, and L is the impactor's diameter. The problem with this scaling relation, however, is that both the impactor's density and diameter—or essentially its mass—must be known. In this study, the natural assumption to make is that the impactor's diameter, L, was 1800 km and the density of the impactor, ρ_i, was ~ 3 g/cm^3. In addition, the density of the target material, ρ_t, was assumed to be that of basalt (3.3 g/cm^3). It is also important to point out that both the Gault scaling law (Eq. (6)) and the π-group scaling law (Eq. (7)) are valid only for incidence angles of 90°. The tacit assumption made is that these relations remain applicable at lower incidence angles. However, the amount of energy imparted to a surface is directly proportional to the sin Θ (Gault and Wedekind, 1978). Essentially these scaling laws were used to estimate the vertical component of the total impact energy. As a result, the masses presented in Table 1 and the impact velocities presented in Table 2 should be taken as lower limits.

2.2. Impact parameters

Resulting values for the total impact energy, W, released during basin formation from Gault's scaling law (Eq. (6)) are listed in Table 1. In order to estimate the mass of the various impactors from these values, three different impact velocities were used: 5, 7, and 10 km/s. These numbers describe the escape velocity of Mars, the minimum impact velocity necessary to vaporize rock (Ahrens and O'Keefe, 1972), and a reasonable velocity of an impacting body with a near-Mars orbit (Davis, 1993), respectively. Two different values for the Borealis basin diameter were used: an average diameter of 9550 km based on Andrews-Hanna et al. (2008) (Borealis A) and, for comparison, the original basin diameter estimate of 7700 km from Wilhelms and Squyres (1984) (Borealis B). In each case the mass of the Borealis impactor is great enough, $\geqslant$0.020 Mars masses (Dones and Tremaine, 1993), to have caused Mars to rotate at its present spin rate. If the impactor that formed the Elysium basin struck Mars at a velocity of 5 km/s, it too may have

Table 1
Martian basin parameters determined using the Gault scaling law. Parameters highlighted in bold are considered possible. Compare with Table 2.

Basin	Diameter (km)	Kinetic energy (10^{36} ergs)	Mars masses			Incidence angles (°)		
			5 km/s	7 km/s	10 km/s	5 km/s	7 km/s	10 km/s
Borealis A	9550	15.5	0.193	0.099	0.048	5	7	10
Borealis B	7700	7.39	0.092	0.047	**0.023**	11	15	**22**
Elysium	4970	1.63	**0.020**	0.010	0.005	**59**	–	–
Daedalia	4500	1.16	0.014	0.007	0.004	–	–	–
Utopia	3300	0.39	0.005	0.003	0.001	–	–	–

Table 2
Martian basin parameters determined using the π-group scaling law. Parameters highlighted in bold are considered possible. Compare with Table 1.

Basin	Diameter (km)	Kinetic energy (10^{36} ergs)	Impact velocity[a] (km/s)	Incidence angles (°)[a]
Borealis A	9550	79.2	40.6	8
Borealis B	7700	29.7	24.9	14
Elysium	4970	4.07	**9.20**	**40**
Daedalia	4500	2.59	**7.34**	**53**
Utopia	3300	0.63	3.63	–

[a] Assumes a mass of 9.6×10^{21} kg.

been massive enough. None of the other impact basins considered in this exercise are large enough.

The resulting value for total impact energy derived from the π-group scaling law was also evaluated. Because the mass of the object is already assumed to be great enough to cause Mars' observed spin, the related impact velocity was determined for each of the known large impact basins (Table 2). Only impact velocities of between 5 and 10 km/s are considered feasible, and thus the estimated velocity of the Borealis impactor in either scenario is too great. However, the π-group scaling law suggests that the Elysium and Daedalia basins are two possibilities. In addition the evidence for the Utopia basin is particularly good (McGill, 1989; Frey and Schultz, 1990), and based on Öpik's theory of close encounters (Öpik, 1976) it may be possible that a near-orbiting object as large as 0.02 Mars masses could encounter Mars at a velocity of ~3.6 km/s (i.e., relative velocity is less than escape velocity), but such a discussion is beyond the scope of this paper. Using either scaling law there appears to be potential impact basins that may have caused Mars' observed spin rate.

One way to determine if any of these values are reasonable is to calculate the incidence angle as a function of mass, velocity, and Mars angular momentum. An assumption made throughout this analysis is that the spin rate of Mars was created by a single impact, which is the simplest scenario. In such a case, the angular momentum contained in the Mars system can be expressed as:

$$L = mrv \sin \Theta \tag{8}$$

where L is the angular momentum, 1.91×10^{39} g cm^2/s, m is the impactor's mass, r is the magnitude of the vector from Mars' center to the impact location (i.e., Mars' radius, or 3.398×10^8 cm), v is the magnitude of the vector impact velocity, and Θ is the angle between r and v, or the incidence angle (Fig. 2). In this equation it is also assumed that the resulting spin is in a prograde direction, so Θ must be between 0 and 90°. From the Gault scaling law, both Borealis impactors at any impact velocity between 5 and 10 km/s and the Elysium impactor at a velocity of 5 km/s yield values for $\sin \Theta$ that are possible. However, many of the predicted masses for the Borealis impactor are more massive than those predicted by either Hartmann and Davis (1975) or Dones and Tremaine (1993). Therefore, only a Borealis impactor with a velocity of 10 km/s (0.023 Mars masses) and the Elysium impactor at a velocity of 5 km/s are considered possible. The π-group scaling law and calculated impact velocities for the Elysium and Daedalia impactors also yield values of Θ that are <90°, so both of these impactors are considered possible. The Utopia impactor yields a value of $\sin \Theta = 1.62$, which is not valid.

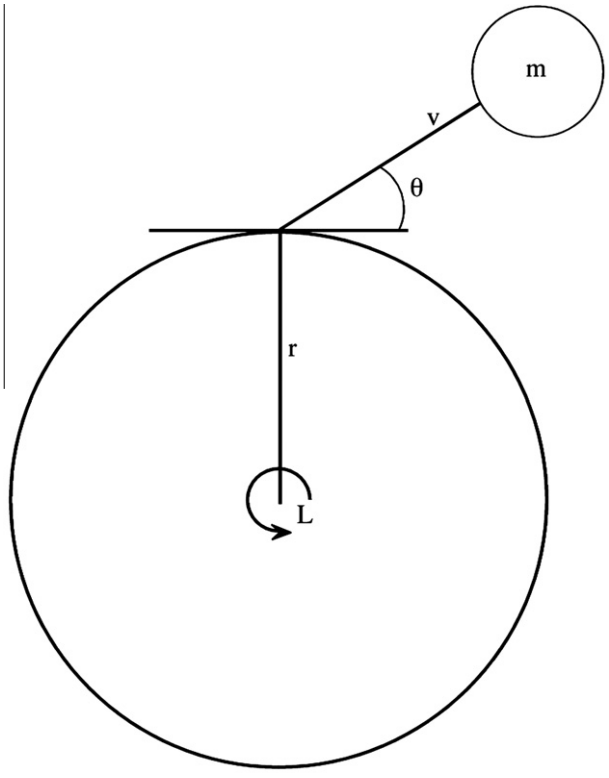

Fig. 2. Diagram describing the variables in Eq. (8). Angular momentum (L) is a function of the mass of the impacting object (m), the length of the vector from Mars' center to the impact location (i.e., the radius of Mars), the impact velocity (v), and the angle between $\vec{r}$ and $\vec{v}$, or the incidence angle (Θ). The predicted size of the Mars-spinning impactor (1800 km; Hartmann and Davis, 1975; Dones and Tremaine, 1993) is to scale with Mars for comparison.

Remarkably, according to calculations based on crater-scaling laws, there appear to be three possibilities for the basin formed by the large impact which presumably caused Mars to spin: Borealis, Elysium, and Daedalia. The evidence for the existence of these basins decreases with increasing size, but one of them may record the largest impact in martian history. Of course this does not preclude the possibility that this large, Mars-spinning impact occurred earlier in martian history than any of these and is not recorded in Mars' surface geology. Crater-scaling laws are crude—especially at the scale of large, basin-forming impacts. Smoothed-particle hydrodynamics (SPH) codes used to simulate the collision of the proto-Earth with the Moon-forming object (e.g., Benz et al., 1986) offer the means to model accurately the physics of shock, vaporization, and transfer of angular momentum, and the estimates presented here provide some initial conditions and constraints for running such simulations. Crater-scaling laws suggest that an object with ~0.02 Mars masses should collide with early Mars at a velocity of between 7 and 10 km/s at an incidence angle of 53–23° (Tables 1 and 2). Future SPH simulations are not only necessary to verify that a large impact could supply the amount of angular momentum in the Mars system, but they are also needed to show that a giant collision could place adequate mass into orbit to form Phobos and Deimos.

3. Formation of Phobos and Deimos

Although somewhat contentious, there is indirect geologic evidence indicating that Mars may have had additional satellites—or moonlets—in the past (Schultz and Lutz-Garihan, 1982, 1988; Schultz, 1985; Strom et al., 1992; Chappelow and Herrick, 2008). This hypothesis is largely predicated on theoretical predictions by Shoemaker (1962) that suggest 0.7% of a planet's impact crater population should be created by a simple, isotropic flux of objects impacting at angles of <5° that would result in elliptical impact craters on the surface. Schultz and Lutz-Garihan (1982) argued that while this is the case for the Moon, they found that Mars has 5–10 times the number of elliptical impact craters than would be predicted from an isotropic flux. They interpret this putative excessive of martian oblique craters to be the result of former satellites whose orbits tidally decayed over time (Schultz and Lutz-Garihan, 1982, 1988; Schultz, 1985; Strom et al., 1992). However, Bottke et al. (2000) conducted a similar survey on the Moon and Mars and found that the population of oblique impact craters is ~5.4% on both planets, which indicates that there is nothing unique about the number of oblique impact craters on Mars. Bottke et al. (2000) argue that oblique craters can form at a much higher threshold angle (<12°) than originally proposed by Shoemaker (1962), suggesting that most of the oblique craters on Mars are simply the natural result of impacting asteroids. There appears to be at least one compelling exception, however. Chappelow and Herrick (2008) demonstrated that a double, oblique impact crater north of Acheron Fossae (Fig. 1) formed when a former Mars-orbiting moonlet collided with Mars. It is possible there are other examples on Mars where this may have occurred as well, but the number of oblique impact craters formed by former moonlets as suggested by Schultz and Lutz-Garihan (1982) would appear to be an extreme.

Interestingly, Schultz and Lutz-Garihan (1982) suggested that the former martian moonlets may have been the result of co-accretion or the breakup of a large captured body. Strom et al. (1992) suggested that material ejected into orbit from the Borealis impact may have formed Phobos and Deimos and additional moonlets. From the calculations presented above, however, it is possible that material could also have been ejected into orbit from either the Elysium or Daedalia impacts as well. Determining the amount and mechanism for placing material into planetary orbit following collision is not straightforward. When a planetary object collides with another a majority of material ejected ballistically from the resulting impact either escapes into space or falls back onto the surface. In order to explain the large amount of material that went into forming the Earth's moon by a giant impact, Cameron and Ward (1976) suggested that large amounts of vaporized material were released during collision. Vaporization allows much more material to be accelerated into orbit than by simple ballistic emplacement (~1/2 the vaporized mass) because the debris is given an added "kick" from pressure gradients on the forward edge of the expanding gas (Cameron, 1986). Vapor from both the planet and impactor need to mix efficiently, however, otherwise vapor from the impactor will exceed escape velocity and vapor from the planet will not reach orbit (Cameron and Ward, 1976). Thus only a narrow set of initial conditions are possible. Low angle (<45°), oblique impacts such as those listed for the Borealis (Table 1) and Elysium (Table 2) impactors also favor the emplacement of vaporized material into orbit as well as jetting, perhaps another important process for inserting material into orbit (Melosh and Sonett, 1986; Melosh, 1984). Low angle impacts would also transfer more angular momentum to Mars than a single, high angle impact. The velocities accompanying these impacts (~10 km/s; Davis, 1993) also exceed the 7 km/s threshold necessary to vaporize rock (Ahrens and O'Keefe, 1972). Following impact, vaporized debris rising above the surface would continue to be accelerated by gas pressure effects and gravity. Obviously the larger than the collision, the more mass that is likely is to be placed into orbit. As described below, however, only a small amount of material from the Mars-spinning impactor had to be inserted into orbit, and large amounts of vaporized material may not be necessary.

3.1. Estimates of inserted mass

Admittedly, any estimate of material inserted into orbit from the impact basins considered in this study is speculative. Obviously with the exception of Phobos and Deimos most of that material is no longer in orbit. However, it is possible to make some estimates as to what was there if it is assumed that oblique craters on the martian surface resulted from the impact of former moonlets as suggested by Schultz and Lutz-Garihan (1982) and more recently by Chappelow and Herrick (2008). On one hand an extreme upper limit can be estimated if it is assumed that all of the 176 oblique impact craters identified by Schultz and Lutz-Garihan (1982) were the result of former moonlets as they suggested (Appendix A). However, as Bottke et al. (2000) demonstrated many of the oblique impact craters considered by Schultz and Lutz-Garihan (1982) are the result of double impact craters or subsequent erosion, or they cannot be confirmed using modern imagery data. A more conservative estimate of the mass of material inserted into martian orbit can be made from the elliptical crater survey conducted by Bottke et al. (2000), which reduces the number of likely oblique craters to only 102 (Appendix B). It should be noted, however, that it is probable that only a fraction of even these craters were made by former moonlets.

Schultz and Lutz-Garihan (1982) calculated the total moonlet mass using a modified π-group scaling relation

$$M = (1.4 \times 10^{-3})\, R^{3.6} \tag{9}$$

where M is the impactor's mass (g) and R is the crater's radius (cm). This equation also attempts to account for the low incidence angles necessary to form an oblique impact crater. They determined a total mass of 1.5×10^{22} g may have been contained in the population of former moonlets, which intuitively appears high. Phobos only has a mass of 1.08×10^{19} g and the total mass determined from their scaling relation would seem to predict that thousands of

Phobos-sized objects were in orbit, which is inconsistent with the number of oblique impact craters they identified on the martian surface (176). However, the diameter of the oblique craters follows a power-law distribution (Appendix A), and the mass differential is accounted for by a few large diameter craters (i.e., moonlets). This scaling relation also predicts that Phobos will eventually form a crater 24 km in diameter. Schultz and Lutz-Garihan (1982) also state that this estimate should be used cautiously since crater-scaling relations are imperfect and not all the oblique impact craters on Mars may be preserved. In contrast, the oblique crater population identified by Bottke et al. (2000) suggests that 4.5×10^{21} g may have been contained in former moonlets, or about a third of the mass suggested by Schultz and Lutz-Garihan (1982).

For comparison, the Gault crater scaling law (Eq. (6)) was applied to the average diameters of both the Schultz and Lutz-Garihan (1982) and Bottke et al. (2000) oblique crater populations by assuming an impact velocity of 5 km/s. This scaling relation estimates the total mass of the Schultz and Lutz-Garihan (1982) moonlet population to be $\sim 6.8 \times 10^{20}$ g and, interestingly, 8.3×10^{20} g for the Bottke et al. (2000) populations. Although there are fewer oblique craters in the Bottke et al. (2000) population, their average diameters are greater than the Schultz and Lutz-Garihan (1982) populations (19.4 km versus 14.6 km, respectively) The Gault crater scaling law also predicts that Phobos will form an impact crater ~53 km across.

The collision between Mars and the Mars-spinning impactor is directly scaled to the collision that took place between the proto-Earth and the Moon-forming impactor: at $\geqslant$1800 km in diameter the Borealis impactor is ~1/4 the diameter of Mars. It is also probable that this planetesimal impacted at a speed meeting or exceeding the velocity needed to vaporize rock. Identical logic has been argued for explaining how so much material was placed into Earth orbit to form the Moon (Cameron, 1986; Melosh and Sonett, 1986; Canup and Esposito, 1995). In the case of the Moon, however, ~10% of the mass of the moon-forming impactor had to go into orbit. In contrast, only a very small fraction of the impactor's mass needs to have been placed into orbit to form Phobos and Deimos and the other putative martian satellites. If either 1.5×10^{22} g or 8.3×10^{20} g of material was contained in the martian satellites, at least twice this amount should have been contained in the accretion disk. Twice the mass is necessary because as the disk dissipated material would move both towards and away from Mars. Only the material that moved away from Mars could go into satellite formation. Taking this into account only ~0.4% or ~0.01% of the mass of the Mars-spinning impactor needs to have gone into orbit around Mars, once again depending upon which scaling law is used. Placing such a small fraction of material into orbit from a giant impact seems entirely plausible. In fact, it may be an unavoidable consequence. Again these estimates are speculative, but they do provide some conditions and constraints for more advanced computer models.

3.2. Satellite formation

It has become widely accepted that the Earth's moon formed from the material inserted into orbit during a collision with a Mars-sized object. However, determining how this material actually goes on to form the Moon remains unclear. It is possible that the Moon was emplaced as a single gravitationally bound clump of material (Stevenson, 1987). Alternatively, the ejected material may form a disk from either a two-phase (liquid-gas) ejecta cloud or from tidal disruption of a clump of material inserted into a highly elliptical orbit (Stevenson, 1987). Initially, Cameron and Ward (1976) and Ward and Cameron (1978) suggested that such a disk would cool rapidly, gravity instabilities would cause the disk to dissipate, and the Moon would form from the cold material spread out past the Roche limit. Thompson and Stevenson (1983, 1988) and Stevenson (1987), however, have calculated that the disk could stay hot as it dissipates, suggesting the possibility that the Moon also formed hot. It is uncertain whether the quantity of material proposed to have been inserted into martian orbit would dissipate as a cold or hot disk. This would essentially depend on how the material was inserted into orbit and in what phase.

Dissipation of the accretion disk could move material beyond the Roche limit of Mars where it could condense and clump together due to gravitational "patch" instabilities. Here the condensed material would coagulate to form small bodies of low mass (Canup and Esposito, 1995, 1996). Stevenson (1987) calculated that the mass of the small bodies that formed from the proto-lunar disk was 10^{20}–10^{22} g (radius of 10–100 km), which is typically more massive than the ancient martian satellites (10^{14}–10^{20} g; Appendices A and B). However, it is not unlikely that smaller satellites would form from the martian disk for a variety of reasons (e.g., different disk densities, sound speeds, orbital angular velocities, etc.). Once these pre-lunar satellites are formed, tidal forces increase the satellites' orbital radii in time proportional to their sizes so larger satellites would recede faster (e.g., Stevenson, 1987). Cameron (1986) and Canup and Esposito (1996) suggested that the last body to form in the Earth–Moon system was more massive than all the rest, so it receded faster and gathered up the smaller satellites that formed earlier; however, calculations by Canup and Esposito (1996) indicate that this is actually difficult to reproduce. Instead, they suggest that a system containing multiple moonlets is a more viable scenario.

In the Earth–Moon system this scenario works because the moonlets also form outside synchronous rotation. Qualitatively, a satellite's orbit grows if its orbital angular velocity, n, is less than the planet's spin, w. Essentially what happens is that the tidal bulge created by the satellite on the planet leads the satellite. A component of the bulge's attraction is in the direction of the satellite's motion, so the satellite speeds up and the orbit expands. This is the typical case for most satellite systems in the Solar System (see Burns, 1986). Why did not the martian satellites use this mechanism to gather into a single massive moon? One possible explanation is the location of the accretion disk relative to the orbit where synchronous rotation occurs. In forming the Mars system, the accretion disk dissipated beyond the Roche limit but stayed mostly within synchronous rotation (Fig. 3). Satellites within synchronous rotation (i.e., $n < w$) lead the bulge they create on the planet's surface. A component of the bulge's attraction is in a direction opposite the satellite's motion, so the satellite slows down and its orbit decays. In this scenario, Deimos is the only satellite to have formed beyond synchronous rotation. Because Phobos appears to be the last satellite waiting to impact on the martian surface (within $\sim 10^8$ years; Dobrovolskis, 1982), it may have formed further out than the others (5.7 Mars radii; Burns, 1992) and/or, as suggested by Appendices A and B, it may have been one of the smallest objects formed. It is also possible that Deimos is actually a combination of smaller satellites that formed beyond synchronous rotation. At Deimos' location, tidal forces would cause the largest object to gather the smaller objects similar to the formation of the Moon. This works closer to Mars as well in that some of the satellites formed within synchronous rotation could have collided with one another to form larger satellites or, alternatively, impact craters on one another (such as Stickney on Phobos) before impacting on the martian surface. It should also be noted that tidal forces would also cause the orbits of the larger satellites to decay faster than the smaller ones causing a certain amount of "sorting" among the satellites. Schultz and Lutz-Garihan (1982) observed that larger diameter oblique impact craters were often the oldest

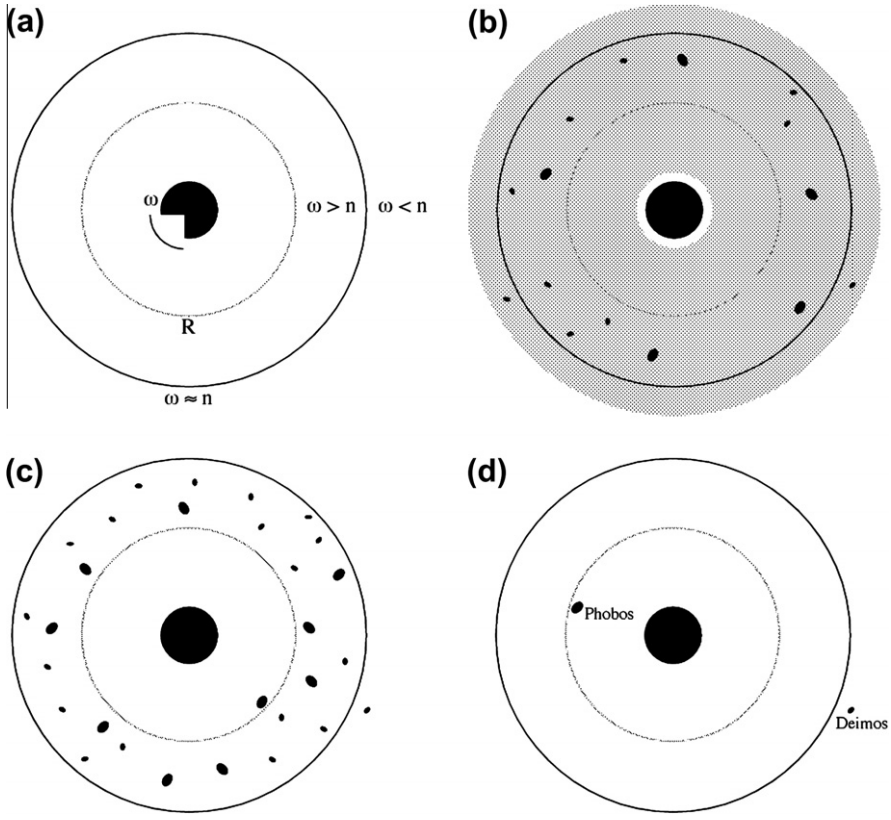

Fig. 3. Plan view of the suggested model for the formation and evolution of the martian satellites and their orbits. (a) The Mars system immediately following the impact of the Mars-spinning object. The planet's spin (ω) has been induced by the collision defining distances where a satellite's orbital angular velocity (n) will be less than, equal to (i.e., synchronous rotation), or greater than the planet's spin. The Roche limit (R) of a small, low-density satellite is also defined. (b) Accretion disk dissipates. Materials dissipated beyond the Roche limit form satellites due to gravitational instabilities within the disk. (c) Initial satellite system. Orbits of the larger satellites formed within synchronous rotation decay quickly due to tides. Orbits of satellites formed beyond synchronous rotation increase. Satellites on either side of synchronous rotation may coalesce with one another. Phobos is the outer, perhaps smallest satellite formed within synchronous rotation. (d) Present martian satellite system after orbital decay of most of the original satellites. Eventually the orbit of Phobos will also decay leaving only Deimos safely beyond synchronous rotation.

indicating that this may have happened. Although this scenario needs to be modeled, it suggests that the accretion disk dissipated quickly and satellite formation occurred soon after; otherwise the orbital decay of the first satellite to form could have disrupted the accretion disk.

3.3. Implications for Phobos, Deimos, and Mars

This hypothesis also has the potential of explaining the physical properties of Phobos and Deimos. The circularity and inclination of the orbits of these satellites would obviously be a holdover from the accretion disk. Their low densities are the result of the accretion disk, but also a function of their small size. The highest gravitational compressive stress experienced in Phobos, the largest of the two, is <100 mbar (10^4 Pa; Dobrovolskis, 1982), hardly enough to melt any type of rock-forming material. The small particles that condensed from the accretion disk coagulated (i.e., aggregated) and remained loosely packed. This would suggest that these objects have a significant amount of pore space. However, this pore space is the direct result of loose aggregation of material, which may have been aided in part by subsequent impact brecciation (Murchie et al., 1991; Fanale and Salvail, 1989, 1990). Such an origin agrees with the libration of Phobos, which indicates that this satellite has a uniform density with depth (Duxbury, 1989). As in the model for the giant impact origin of the Earth's moon (Cameron, 1985, 1986; Wood, 1986) vaporization of material would fractionate elements according to their volatility. Thus, Phobos and Deimos are expected to be depleted in low temperature volatile elements, such as water. In the model presented here, the low densities of these moons could not be explained by a substantial component of water ice as suggested by Fanale and Salvail (1989, 1990) but instead would be due to their status as a "rubble pile" of material (e.g., Singer, 2007). This is also supported by the lack of a strong hydration signature in the 3-mm band measured by the Phobos 2 ISM experiment (Langevin et al., 1990) and Earth-based telescopic observations (Rivkin et al., 2002). Potentially the composition of Phobos and Deimos would depend primarily upon the composition of the large impactor and not the composition of Mars, since in the Earth–Moon system it is predicted that a majority of the mass inserted into orbit came from the Mars-sized impactor and not the proto-Earth (Cameron, 1986, Melosh and Sonett, 1986).

Finally, Schultz and Lutz-Garihan (1982, 1988) and Schultz (1985) interpreted the change in orientation of the martian elongated craters with different-age geologic units as being the result of polar wandering. That is, the martian crust presently at higher latitudes was once near the rotational equator and has shifted with time. Alternatively, the oblique impact crater population may record the formation of the Tharsis bulge, which is thought to have reoriented the lithosphere of Mars by as much as 25° (Melosh, 1980; Willemann, 1984). In addition, the formation of the Tharsis bulge would have caused the orbital plane of the satellites to precess over time, if the satellites were still present as the Tharsis bulge was forming. It is this influence that may also be recorded, in part, in the martian oblique crater population.

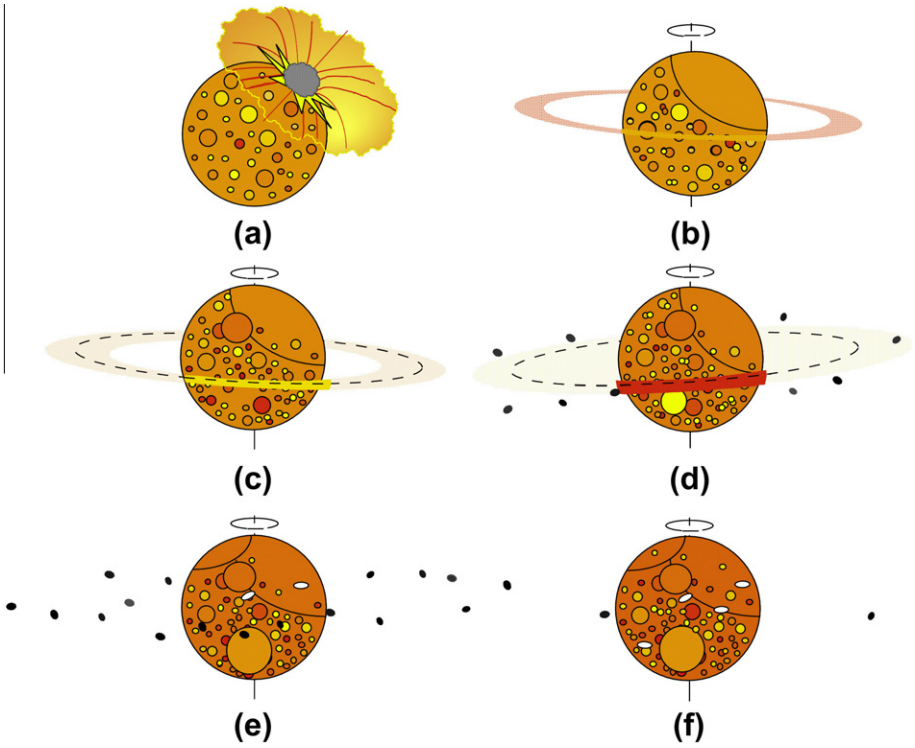

Fig. 4. Model for the origin of Phobos and Deimos. (a) Mars-spinning planetesimal collides with Mars vaporizing material and associated large impact basin is formed. Angular momentum imparted to the surface gives Mars its final spin rate. (b) Vaporized material forms an accretionary disk. (c) Materials dissipate past the Roche limit of Mars (dashed line) and begin to coalesce into small moons. (d) Moons continue to form until accretion disk is exhausted. Only Deimos forms outside synchronous rotation. (e) Accretion disk completely dissipates. Dozens of small moons are left orbiting Mars. Tidal perturbations cause these moons to fall back towards the martian surface forming grazing impacts (white ellipses). Development of the Tharsis bulge causes the orbital plane to precess. (f) Present martian system with only Phobos and Deimos in orbit.

4. Summary

Are Phobos and Deimos the result of a giant impact? Numerous observations support the hypothesis that they are:

(1) Because Mars excess much prograde angular momentum, it may have collided with an object that was 0.02 its mass (Dones and Tremaine, 1993). Such an object near the orbit of Mars is also predicted by accretionary theory calculations performed by Hartmann and Davis (1975), which originally inspired the giant impact hypothesis for forming the Moon. It appears from current crater-scaling laws that the giant impact impact on Mars may have occurred after formation of the crust and created the topographic dichotomy in hemispheres (Wilhelms and Squyres, 1984; Andrews-Hanna et al., 2008), but such an impact may have also created the Elysium (Frey and Schultz, 1990) or Daedalia (Craddock et al., 1990) impact basins. The impact velocity of this Mars-spinning object may have been great enough to vaporize rock, thus helping insert material into orbit.

(2) It has been suggested that oblique impact craters on Mars record the slow orbital decay of ancient moonlets (Schultz and Lutz-Garihan, 1982, 1988; Schultz, 1985; Chappelow and Herrick, 2008). Assuming that all or at least a fraction of oblique impact craters on Mars resulted from the impact of former moonlets, the total mass that may have been inserted into orbit from the giant collision that formed these satellites is $\sim 10^{22}$ to $\sim 10^{21}$ g. This is only a small fraction of the mass of the Mars-spinning object (<0.5%), and it is thus plausible that Mars once had an impact-generated accretion disk.

(3) The hypothesis that Phobos and Deimos formed as a result of a giant impact early in martian history has merit in that it explains the physical properties of these satellites better or at least as well as any other hypothesis proposed previously. Fig. 4 summarizes the sequence of events that describe the giant impact hypothesis.

Support for the origin of the Earth's moon by a giant impact comes from sophisticated numerical models such as smoothed-particle hydrodynamics (e.g., Cameron and Benz, 1991) and other codes (e.g., Canup and Esposito, 1995). These models illustrate the possibility of inserting the necessary material into orbit to form the Moon; however, they represent time consuming, arduous tasks. Simple cratering laws applied to the larger, albeit putative martian basins provide information on the initial conditions and constraints needed for such simulations (Tables 1 and 2), which will be useful in testing the giant impact hypothesis. Ultimately, however, better compositional information from both remote sensing data and returned samples will also be needed to further our understanding of the martian moons and possibly the formation of the Earth–Moon system as well.

Acknowledgments

I thank Erik Asphaug, Bruce Campbell, Alan Howard, Jay Melosh, Trish Campbell, Steve Soter, and Jim Zimbelman for many useful discussions. Special thanks to Luke Dones for his tireless encouragement and to Bill Bottke for sharing his oblique crater database. Thanks also to Ana Baptista and Nicolas Mangold for their support. Two anonymous reviewers provided many constructive comments and suggestions for improving the original manuscript. Finally, "Merry Christmas, Mister Potter!"

Appendix A

Masses of bolides needed to create oblique impact craters listed by Schultz and Lutz-Garihan (1988) based on π-group scaling (Eq. (9)) and Gault scaling (Eq. (6)) laws. Mass of Phobos (P) and Deimos (D) are given for comparison. The crater resulting from the eventual impact of Phobos on Mars is also listed to illustrate the differences in scaling laws.

Maximum diameter (km)	Minimum diameter (km)	π-Group mass (g)	Gault mass (g)
140	50	1.5×10^{21}	3.0×10^{20}
95	50	5.7×10^{20}	8.6×10^{19}
88	47	4.4×10^{20}	6.6×10^{19}
74	52	3.5×10^{20}	4.2×10^{19}
70	30	1.5×10^{20}	2.8×10^{19}
68	25	1.2×10^{20}	2.5×10^{19}
62	51	2.3×10^{20}	2.7×10^{19}
60	42	1.6×10^{20}	2.0×10^{19}
	53	–	1.1×10^{19} (P)
50	25	5.4×10^{19}	9.2×10^{18}
45	28	4.9×10^{19}	7.0×10^{18}
44	30	5.1×10^{19}	6.9×10^{18}
42	32	5.1×10^{19}	6.4×10^{18}
40	25	3.2×10^{19}	4.7×10^{18}
40	30	4.2×10^{19}	5.4×10^{18}
34	15	1.2×10^{19}	2.4×10^{18}
33	28	2.5×10^{19}	3.2×10^{18}
32	30	2.7×10^{19}	3.3×10^{18}
		–	1.8×10^{18} (D)
30	19	1.2×10^{19}	1.7×10^{18}
30	18	1.1×10^{19}	1.7×10^{18}
30	25	1.8×10^{19}	2.2×10^{18}
23		1.1×10^{19} (P)	–
30	10	5.6×10^{18}	1.5×10^{18}
30	10	5.6×10^{18}	1.5×10^{18}
29	28	2.0×10^{19}	2.4×10^{18}
28	10	4.6×10^{18}	1.2×10^{18}
26	16	6.6×10^{18}	1.1×10^{18}
25	10	3.4×10^{18}	8.1×10^{17}
25	18	7.2×10^{18}	1.0×10^{18}
24	10	3.1×10^{18}	7.0×10^{17}
24	16	5.6×10^{18}	8.4×10^{17}
23	12	3.4×10^{18}	6.4×10^{17}
22	20	6.6×10^{18}	8.6×10^{17}
22	17	5.1×10^{18}	7.0×10^{17}
21	15	3.8×10^{18}	5.6×10^{17}
21	15	3.8×10^{18}	5.6×10^{17}
20	15	3.4×10^{18}	4.9×10^{17}
20	20	5.6×10^{18}	7.2×10^{17}
20	16	3.8×10^{18}	5.2×10^{17}
20	19	5.1×10^{18}	6.6×10^{17}
20	18	4.6×10^{18}	6.1×10^{17}
20	18	4.6×10^{18}	6.1×10^{17}
20	18	4.6×10^{18}	6.1×10^{17}
20	12	2.5×10^{18}	4.2×10^{17}
20	15	3.4×10^{18}	4.9×10^{17}
20	18	4.6×10^{18}	6.1×10^{17}
19	17	3.8×10^{18}	5.0×10^{17}
19	14	2.8×10^{18}	4.0×10^{17}
19	18	4.2×10^{18}	5.5×10^{17}
19	11	2.0×10^{18}	3.5×10^{17}
18	11	1.8×10^{18}	2.9×10^{17}
18	15	2.8×10^{18}	3.8×10^{17}
18	10	1.5×10^{18}	2.8×10^{17}
18	12	2.0×10^{18}	3.1×10^{17}
17	14	2.2×10^{18}	3.1×10^{17}
		1.8×10^{18} (D)	–
17	11	1.5×10^{18}	2.5×10^{17}
16	10	1.2×10^{18}	2.0×10^{17}
16	12	1.5×10^{18}	2.3×10^{17}
16	10	1.2×10^{18}	2.0×10^{17}
15	4	3.8×10^{17}	1.3×10^{17}
15	10	1.0×10^{18}	1.7×10^{17}
15	13	1.5×10^{18}	2.1×10^{17}
15	13	1.5×10^{18}	2.1×10^{17}
15	11	1.2×10^{18}	1.8×10^{17}
15	13	1.5×10^{18}	2.1×10^{17}
15	12	1.4×10^{18}	1.9×10^{17}
15	12	1.4×10^{18}	1.9×10^{17}
15	13	1.5×10^{18}	2.1×10^{17}
15	12	1.4×10^{18}	1.9×10^{17}
15	3	3.1×10^{17}	1.3×10^{17}
14	11	1.0×10^{18}	1.5×10^{17}
14	11	1.0×10^{18}	1.5×10^{17}
14	8	6.5×10^{17}	1.2×10^{17}
14	11	1.0×10^{18}	1.5×10^{17}
14	10	8.9×10^{17}	1.4×10^{17}
14	12	1.2×10^{18}	1.7×10^{17}
13	5	3.1×10^{17}	8.4×10^{16}
13	10	7.6×10^{17}	1.1×10^{17}
12	11	7.6×10^{17}	1.1×10^{17}
12	10	6.5×10^{17}	9.4×10^{16}
12	11	7.6×10^{17}	1.1×10^{17}
12	10	6.5×10^{17}	9.4×10^{16}
12	10	6.5×10^{17}	9.4×10^{16}
12	10	6.5×10^{17}	9.4×10^{16}
12	8	4.6×10^{17}	7.7×10^{16}
12	11	7.6×10^{17}	1.1×10^{17}
12	7	3.8×10^{17}	7.1×10^{16}
12	10	6.5×10^{17}	9.4×10^{16}
12	9	5.5×10^{17}	8.4×10^{16}
12	6	3.1×10^{17}	6.7×10^{16}
12	10	6.5×10^{17}	9.4×10^{16}
11	8	3.8×10^{17}	6.1×10^{16}
11	10	5.5×10^{17}	7.8×10^{16}
11	9	4.6×10^{17}	6.8×10^{16}
11	10	5.5×10^{17}	7.8×10^{16}
11	10	5.5×10^{17}	7.8×10^{16}
11	8	3.8×10^{17}	6.1×10^{16}
11	9	4.6×10^{17}	6.8×10^{16}
11	9	4.6×10^{17}	6.8×10^{16}
10	5	1.6×10^{17}	3.6×10^{16}
10	8	3.1×10^{17}	4.8×10^{16}
10	6	2.1×10^{17}	3.8×10^{16}
10	9	3.8×10^{17}	5.6×10^{16}
10	9	3.8×10^{17}	5.6×10^{16}
10	8	3.1×10^{17}	4.8×10^{16}
10	6	2.1×10^{17}	3.8×10^{16}
10	9	3.8×10^{17}	5.6×10^{16}
10	9	3.8×10^{17}	5.6×10^{16}
10	5	1.6×10^{17}	3.6×10^{16}
10	3	9.7×10^{16}	3.3×10^{16}
10	6	2.1×10^{17}	3.8×10^{16}

Appendix A (*continued*)

Maximum diameter (km)	Minimum diameter (km)	π-Group mass (g)	Gault mass (g)
10	8	3.1×10^{17}	4.8×10^{16}
10	6	2.1×10^{17}	3.8×10^{16}
10	9	3.8×10^{17}	5.6×10^{16}
10	5	1.6×10^{17}	3.6×10^{16}
10	8	3.1×10^{17}	4.8×10^{16}
10	10	4.6×10^{17}	6.6×10^{16}
10	8	3.1×10^{17}	4.8×10^{16}
10	8	3.1×10^{17}	4.8×10^{16}
10	10	4.6×10^{17}	6.6×10^{16}
10	9	3.8×10^{17}	5.6×10^{16}
10	10	4.6×10^{17}	6.6×10^{16}
10	9	3.8×10^{17}	5.6×10^{16}
10	10	4.6×10^{17}	6.6×10^{16}
10	8	3.1×10^{17}	4.8×10^{16}
10	8	3.1×10^{17}	4.8×10^{16}
10	8	3.1×10^{17}	4.8×10^{16}
10	8	3.1×10^{17}	4.8×10^{16}
10	7	2.6×10^{17}	4.2×10^{16}
10	9	3.8×10^{17}	5.6×10^{16}
10	9	3.8×10^{17}	5.6×10^{16}
9	6	1.6×10^{17}	2.8×10^{16}
9	8	2.6×10^{17}	3.8×10^{16}
9	7	2.1×10^{17}	3.2×10^{16}
9	6	1.6×10^{17}	2.8×10^{16}
9	7	2.1×10^{17}	3.2×10^{16}
9	8	2.6×10^{17}	3.8×10^{16}
9	6	1.6×10^{17}	2.8×10^{16}
9	7	2.1×10^{17}	3.2×10^{16}
9	8	2.6×10^{17}	3.8×10^{16}
9	8	2.6×10^{17}	3.8×10^{16}
9	9	3.1×10^{17}	4.6×10^{16}
9	5	1.3×10^{17}	2.6×10^{16}
9	8	2.6×10^{17}	3.8×10^{16}
9	8	2.6×10^{17}	3.8×10^{16}
9	7	2.1×10^{17}	3.2×10^{16}
9	5	1.3×10^{17}	2.6×10^{16}
8	6	1.3×10^{17}	2.1×10^{16}
8	6	1.3×10^{17}	2.1×10^{16}
8	6	1.3×10^{17}	2.1×10^{16}
8	5	9.7×10^{16}	1.8×10^{16}
8	8	2.1×10^{17}	3.0×10^{16}
8	5	9.7×10^{16}	1.8×10^{16}
8	8	2.1×10^{17}	3.0×10^{16}
8	4	7.3×10^{16}	1.7×10^{16}
8	7	1.6×10^{17}	2.5×10^{16}
8	4	7.3×10^{16}	1.7×10^{16}
7	3	3.8×10^{16}	1.0×10^{16}
7	6	9.7×10^{16}	1.5×10^{16}
7	3	3.8×10^{16}	1.0×10^{16}
7	6	9.7×10^{16}	1.5×10^{16}
7	3	3.8×10^{16}	1.0×10^{16}
7	3	3.8×10^{16}	1.0×10^{16}
7	6	9.7×10^{16}	1.5×10^{16}
6	2	1.7×10^{16}	5.8×10^{15}
6	4	3.8×10^{16}	7.0×10^{15}
6	5	5.3×10^{16}	8.6×10^{15}
6	5	5.3×10^{16}	8.6×10^{15}
6	4	3.8×10^{16}	7.0×10^{15}
5	5	3.8×10^{16}	6.0×10^{15}
5	3	1.7×10^{16}	3.5×10^{15}

Appendix A (*continued*)

Maximum diameter (km)	Minimum diameter (km)	π-Group mass (g)	Gault mass (g)
5	3	1.7×10^{16}	3.5×10^{15}
5	3	1.7×10^{16}	3.5×10^{15}
4	2	6.0×10^{15}	1.5×10^{15}
4	2	6.0×10^{15}	1.5×10^{15}
4	3	1.0×10^{16}	1.9×10^{15}
3	2	3.1×10^{15}	6.4×10^{14}
2	2	1.4×10^{15}	2.6×10^{14}

Appendix B

Masses of bolides needed to create the "likely" oblique impact craters listed by Bottke et al. (2000) based on π-group scaling (Eq. (9)) and Gault scaling (Eq. (6)) laws.

Maximum diameter (km)	Minimum diameter (km)	π-Group mass (g)	Gault mass (g)
40	30	4.2×10^{19}	5.4×10^{18}
10	9	3.8×10^{17}	5.6×10^{16}
12.2	6.7	3.7×10^{17}	7.3×10^{16}
20	18	4.6×10^{18}	6.1×10^{17}
10	8	3.1×10^{17}	4.8×10^{16}
9	7	2.1×10^{17}	3.2×10^{16}
9	5	1.3×10^{17}	2.6×10^{16}
10	7	2.6×10^{17}	4.2×10^{16}
23.7	18.3	6.6×10^{18}	9.1×10^{17}
23.5	11.3	3.4×10^{18}	6.7×10^{17}
48	25.2	4.9×10^{19}	8.1×10^{18}
17	11	1.5×10^{18}	2.5×10^{17}
15.8	10.6	1.2×10^{18}	2.0×10^{17}
8	7	1.6×10^{17}	2.5×10^{16}
53.2	26.3	6.6×10^{19}	1.1×10^{19}
10	8	3.1×10^{17}	4.8×10^{16}
31.1	16.2	1.0×10^{19}	1.8×10^{18}
30	18	1.1×10^{19}	1.7×10^{18}
33.4	19.9	1.6×10^{19}	2.5×10^{18}
35	18	1.5×10^{19}	2.7×10^{18}
13	7.8	5.3×10^{17}	9.5×10^{16}
11.7	6.3	3.1×10^{17}	6.3×10^{16}
42.5	25.2	3.7×10^{19}	5.6×10^{18}
44	30	5.1×10^{19}	6.9×10^{18}
42.2	27.1	4.0×10^{19}	5.7×10^{18}
9.8	6.2	2.1×10^{17}	3.7×10^{16}
29.1	18.7	1.1×10^{19}	1.6×10^{18}
30	25	1.8×10^{19}	2.2×10^{18}
137.7	42.9	1.3×10^{21}	2.8×10^{20}
140	50	1.5×10^{21}	3.0×10^{20}
30	19	1.2×10^{19}	1.7×10^{18}
26	16	6.6×10^{18}	1.1×10^{18}
9	7	2.1×10^{17}	3.2×10^{16}
13.4	6.6	4.6×10^{17}	9.8×10^{16}
11	8	3.8×10^{17}	6.1×10^{16}
12	9	5.5×10^{17}	8.4×10^{16}
15.9	8.5	9.4×10^{17}	1.8×10^{17}
10.6	6.2	2.5×10^{17}	4.6×10^{16}
15	12	1.4×10^{18}	1.9×10^{17}
10	6	2.1×10^{17}	3.8×10^{16}
14	8.3	6.8×10^{17}	1.2×10^{17}

(*continued on next page*)

Appendix B (*continued*)

Maximum diameter (km)	Minimum diameter (km)	π-Group mass (g)	Gault mass (g)
14	11	1.0×10^{18}	1.5×10^{17}
11	10	5.5×10^{17}	7.8×10^{16}
10	8	3.1×10^{17}	4.8×10^{16}
9.2	6.4	1.9×10^{17}	3.2×10^{16}
19	11	2.0×10^{18}	3.5×10^{17}
20	18	4.6×10^{18}	6.1×10^{17}
26.8	20.1	9.9×10^{18}	1.3×10^{18}
10	8	3.1×10^{17}	4.8×10^{16}
18.3	11.5	1.9×10^{18}	3.2×10^{17}
28.9	23.7	1.5×10^{19}	1.9×10^{18}
13	9.1	6.6×10^{17}	1.0×10^{17}
15	12	1.4×10^{18}	1.9×10^{17}
18.8	11.9	2.1×10^{18}	3.5×10^{17}
20	15	3.4×10^{18}	4.9×10^{17}
12	10	6.5×10^{17}	9.4×10^{16}
10	9	3.8×10^{17}	5.6×10^{16}
22	20	6.6×10^{18}	8.6×10^{17}
21.3	13.7	3.4×10^{18}	5.4×10^{17}
10	6	2.1×10^{17}	3.8×10^{16}
27.9	23.6	1.4×10^{19}	1.8×10^{18}
18	11	1.8×10^{18}	2.9×10^{17}
40.3	26.4	3.5×10^{19}	4.9×10^{18}
14.6	7.1	6.2×10^{17}	1.3×10^{17}
36.8	25.4	2.7×10^{19}	3.7×10^{18}
16	10	1.2×10^{18}	2.0×10^{17}
9	7	2.1×10^{17}	3.2×10^{16}
24	16	5.6×10^{18}	8.4×10^{17}
22.9	14.6	4.4×10^{18}	6.9×10^{17}
12	10	6.5×10^{17}	9.4×10^{16}
15	13	1.5×10^{18}	2.1×10^{17}
21.2	12.6	3.0×10^{18}	5.1×10^{17}
23	12	3.4×10^{18}	6.4×10^{17}
15.2	11	1.2×10^{18}	1.8×10^{17}
18.7	9.4	1.6×10^{18}	3.1×10^{17}
16.4	11.1	1.4×10^{18}	2.3×10^{17}
18	15	2.8×10^{18}	3.8×10^{17}
10	6	2.1×10^{17}	3.8×10^{16}
15	13	1.5×10^{18}	2.1×10^{17}
33	28	2.5×10^{19}	3.2×10^{18}
50	25	5.4×10^{19}	9.2×10^{18}
14	11	1.0×10^{18}	1.5×10^{17}
15	11	1.2×10^{18}	1.8×10^{17}
15.5	11.9	1.4×10^{18}	2.1×10^{17}
21	15	3.8×10^{18}	5.6×10^{17}
16.8	8.4	1.1×10^{18}	2.1×10^{17}
16	10	1.2×10^{18}	2.0×10^{17}
88	47	4.4×10^{20}	6.6×10^{19}
81.8	46.1	3.7×10^{20}	5.2×10^{19}
9	7	2.1×10^{17}	3.2×10^{16}
20.7	13.9	3.3×10^{18}	5.1×10^{17}
19.8	13.8	3.0×10^{18}	4.5×10^{17}
20	18	4.6×10^{18}	6.1×10^{17}
21.4	14.7	3.9×10^{18}	5.8×10^{17}
19	14	2.8×10^{18}	4.0×10^{17}
9	8	2.6×10^{17}	3.8×10^{16}
17.3	11.3	1.7×10^{18}	2.7×10^{17}
11.1	6.6	3.0×10^{17}	5.5×10^{16}
62	51	2.3×10^{20}	2.7×10^{19}
24	10	3.1×10^{18}	7.0×10^{17}
24.8	10	3.4×10^{18}	7.8×10^{17}
19.6	8.9	1.6×10^{18}	3.6×10^{17}

References

Ahrens, T.J., O'Keefe, J.D., 1972. Shock melting and vaporization of lunar rocks and minerals. Moon 4, 214–219.

Andrews-Hanna, J.C., Zuber, M.T., Banerdt, W.B., 2008. The Borealis Basin and the origin of the martian crustal dichotomy. Nature 453, 1212–1215.

Asphaug, E., Benz, W., 1994. The surface and interior of Phobos. Lunar Planet. Sci. XXV, 43–44.

Benz, W., Slattery, W.L., Cameron, A.G.W., 1986. The origin of the Moon and the single-impact hypothesis I. Icarus 66, 515–535.

Bottke, W.F., Love, S.G., Tytell, D., Glotch, T., 2000. Interpreting the elliptical crater populations on Mars, Venus, and the Moon. Icarus 145, 108–121.

Burns, J.A., 1978. On the orbital evolution and origin of the martian moons. Vistas Astron. 22, 193–210.

Burns, J.A., 1986. The evolution of satellite orbits. In: Burns, J.A., Matthews, M.S. (Eds.), Satellites. Univ. Arizona Press, Tucson, pp. 117–158.

Burns, J.A., 1992. Contradictory clues as to the origin of the martian moons. In: Kieffer, H.H., Jakosky, B.M., Snyder, C.W., Matthews, M.S. (Eds.), Mars. Univ. Arizona Press, Tucson, pp. 1283–1301.

Cameron, A.G.W., 1985. Formation of the pre-lunar accretion disk. Icarus 62, 319–327.

Cameron, A.G.W., 1986. The impact theory for origin of the Moon. In: Hartmann, W.K., Phillips, R.J., Taylor, G.J. (Eds.), Origin of the Moon. Lunar and Planetary Institute, Houston, pp. 609–616.

Cameron, A.G.W., Benz, W., 1991. The origin of the Moon and the single impact hypothesis IV. Icarus 92, 204–216.

Cameron, A.G.W., Ward, W., 1976. The origin of the Moon. Lunar Planet. Sci. VII, 120–121.

Canup, R.M., Esposito, L.W., 1995. Accretion in the Roche Zone: Co-existence of rings and ringmoons. Icarus 113, 331–352.

Canup, R.M., Esposito, L.W., 1996. Accretion of the Moon from and impact-generated disk. Icarus 119, 427–446.

Chappelow, J.E., Herrick, R.R., 2008. On the origin of a double, oblique impact on Mars. Icarus 197, 452–457.

Craddock, R.A., Greeley, R., Christensen, P.R., 1990. Evidence for an ancient impact basin in Daedalia Planum, Mars. J. Geophys. Res. 95, 10729–10741.

Davis, P.M., 1993. Meteoroid impacts as seismic sources on Mars. Icarus 105, 469–478.

Dobrovolskis, A.R., 1982. Internal stresses in Phobos and other triaxial bodies. Icarus 5, 136–148.

Dones, L., Tremaine, S., 1993. Why does the Earth spin forward? Science 259, 350–354.

Duxbury, T.C., 1989. The figure of Phobos. Icarus 78, 169–180.

Fanale, F.P., Salvail, J.R., 1989. Loss of water from Phobos. Geophys. Res. Lett. 16, 287–290.

Fanale, F.P., Salvail, J.R., 1990. Evolution of the water regime of Phobos. Icarus 88, 380–395.

Forget, F., Costard, F., Lognonne, P., 2008. Planet Mars, Story of Another World. Spinger Praxis Books, Chichester, United Kingdom, 229 pp.

Frey, H., Schultz, R.A., 1988. Large impact basins and the mega-impact origin for the crustal dichotomy on Mars. Geophys. Res. Lett. 15, 229–232.

Frey, H., Schultz, R.A., 1990. Speculations on the origin and evolution of the Utopia–Elysium lowlands of Mars. J. Geophys. Res. 95, 14203–14213.

Gault, D.E., 1974. Impact cratering. In: Greeley, R., Schultz, P.H. (Eds.), A Primer in Lunar Geology. NASA Ames, Moffett Field, pp. 137–175.

Gault, D.E., Wedekind, J.A., 1977. Experimental hypervelocity impact into quartz sand – II: Effects of gravitational acceleration. In: Roddy, D.J., Pepin, R.O., Merrill, R.B. (Eds.), Impact and Explosion Cratering. Pergamon, New York, pp. 1231–1244.

Gault, D.E., Wedekind, J.A., 1978. Experimental studies of oblique impact. Proc. Lunar Sci. Conf. 9, 3843–3875.

Hartmann, W.K., Davis, D.R., 1975. Satellite-sized planetesimals and lunar origin. Icarus 24, 504–515.

Hartmann, W.K., Davis, D.R., Chapman, C.R., Soter, S., Greenberg, R., 1975. Mars: Satellite origin and angular momentum. Icarus 25, 588–594.

Holsapple, K.A., Schmidt, R.M., 1980. On the scaling of crater dimensions: 1, Explosive processes. J. Geophys. Res. 85, 7247–7256.

Holsapple, K.A., Schmidt, R.M., 1982. On the scaling of crater dimensions: 2, Impact processes. J. Geophys. Res. 87, 1849–1870.

Housen, K.R., Wilkening, L.L., Chapman, C.R., Greenberg, R., 1979. Asteroidal regoliths. Icarus 39, 317–351.

Lambeck, K., 1979. On the orbital evolution of the martian satellites. J. Geophys. Rev. 84, 5651–5658.

Landis, L.G., 2002. Origin of Martian Moons from Binary Asteroid Dissociation. presented at the AAAS Annual Meeting, February 14–19, Boston MA.

Langevin, Y., Bibring, J.P., Gondet, B., Combes, M., Grigoriev, A.V., Joukov, B., Nikolsky, Y.V., 1990. Observations of Phobos from 0.8 to 3.15 mm with the ISM experiment on board the Soviet "Phobos II" spacecraft. Lunar Planet. Sci. XXI, 682–683.

Lynch, D.K., Russell, R.W., Rudy, R.J., Mazuk, S., Venturini, C.C., Hammel, H.B., Sykes, M.V., Puetter, R.C., Perry, R.B., 2007. Infrared spectra of Deimos (1–13 μm) and Phobos (3–13 μm). Astronomical Journal 134, 1459–1463.

McGill, G.E., 1989. Buried topography of Utopia, Mars: Persistence of a giant impact depression. J. Geophys. Res. 94, 2753–2759.

McGill, G.E., Squyres, S.W., 1991. Origin of the martian crustal dichotomy: Evaluating hypotheses. Icarus 93, 386–393.

Melosh, H.J., 1980. Tectonic patterns on a reoriented planet: Mars. Icarus 44, 745–751.
Melosh, H.J., 1984. Impact ejection, spallation and the origin of meteorites. Icarus 59, 234–260.
Melosh, H.J., 1989. Impact Cratering, A Geologic Process. Oxford University Press, New York. 245pp.
Melosh, H.J., Sonett, C.P., 1986. When worlds collide: Jetted vapor plumes and the Moon's origin. In: Hartmann, W.K., Phillips, R.J., Taylor, G.J. (Eds.), Origin of the Moon. Lunar and Planetary Institute, Houston, pp. 621–642.
Murchie, S.L. et al., 1991. Color heterogeneity of the surface of Phobos: Relationship to geologic features and comparisons to meteorite analogs. J. Geophys. Res. 96, 5925–5945.
Nordyke, M.D., 1962. An analysis of cratering data from desert alluvium. J. Geophys. Res. 67, 1965–1974.
Öpik, E.J., 1976. Interplanetary Encounters. Elsevier, New York. 155pp.
Pollack, J.B., Burns, J.A., Tauber, M.E., 1979. Gas drag in primordial circumplanetary envelopes: A mechanism for satellite capture. Icarus 37, 587–611.
Rivkin, A.S., Brown, R.H., Trilling, D.E., Bell III, J.F., Plassman, J.F., 2002. Near-infrared spectrometry of Phobos and Deimos. Icarus 156, 64–75.
Rosenblatt, P., Le Maistre, S., Marty, J., Dehant, V., Paetzold, M., van Hoolst, T., 2008. Improvement of the Mass Determination of Both Martian Moons Using MEX, MGS, ODY and MRO Tracking Data, American Geophysical Union, Fall Meeting 2008, abstract #P41B-1377.
Safronov, V.S., Pechernikova, G.V., Ruskol, E.L., Vitjazev, A.V., 1986. Protosatellites swarms. In: Burns, J.A., Matthews, M.S. (Eds.), Satellites. Univ. Arizona Press, Tucson, pp. 89–116.
Schultz, P.H., 1985. Polar wandering on Mars. Sci. Am. 253, 94–102.
Schultz, R.A., Frey, H.V., 1990. A new survey of large multiring impact basins on Mars. J. Geophys. Res. 95, 14175–14189.
Schultz, P.H., Lutz-Garihan, A.B., 1982. Grazing impacts on Mars: A record of lost satellites. Proc. Lunar Sci. Conf. 13, J. Geophys. Res. Suppl. 87, A84–A96.
Schultz, P.H., Lutz-Garihan, A.B., 1988. Polar wandering on Mars. Icarus 73, 91–141.
Shoemaker, E.M., 1962. Interpretation of lunar craters. In: Kopal, Z. (Ed.), Physics and Astronomy of the Moon. Academic Press, New York, pp. 283–359.
Singer, S.F., 1966. On the origin of the martian satellites Phobos and Deimos. In: Dollfus, A. (Ed.), Moon and Planets, COSPAR Seventh Int. Space Sci. Symp., Vienna, pp. 317–321.
Soter, S., 1971. The Dust Belts of Mars. Cornell University Center for Radiophysics and Space Research, Report No. 462.
Singer, S.F., 2007. Origin of the Martian satellites Phobos and Deimos, Workshop on the Exploration of Phobos and Deimos, abstract 7020, Lunar and Planetary Institute, Houston, Texas.
Stevenson, D.J., 1987. Origin of the Moon – The collision hypothesis. Annu. Rev. Earth Planet. Sci. 15, 271–315.
Strom, R.G., Croft, S.K., Barlow, N.G., 1992. The martian impact cratering record. In: Kieffer, H.H., Jakosky, B.M., Snyder, C.W., Matthews, M.S. (Eds.), Mars. Univ. Arizona Press, Tucson, pp. 383–423.
Thompson, C., Stevenson, D.J., 1983. Two-phase gravitational instabilities in thin disks with application to the origin of the Moon. Lunar Planet. Sci. XIV, 787–788.
Thompson, C., Stevenson, D.J., 1988. Gravitational instability in two-phase disks and the origin of the Moon. Astrophys. J. 333, 452–481.
Ward, W.R., Cameron, A.G.W., 1978. Disc evolution within the Roche limit. Lunar Planet. Sci. IX, 1205–1206.
Wilhelms, D.E., Squyres, S.W., 1984. The martian hemispheric dichotomy may be due to a giant impact. Nature 309, 138–140.
Willemann, R.J., 1984. Reorientation of planets with elastic lithospheres. Icarus 60, 701–709.
Wood, J.A., 1986. Moon over Mauna Loa: A review of hypotheses of formation of Earth's moon, review paper. In: Hartmann, W.K., Phillips, R.J., Taylor, G.J. (Eds.), Origin of the Moon. Lunar and Planetary Institute, Houston, pp. 17–55.